

EPISODIC STARBURSTS IN DWARF SPHEROIDAL GALAXIES: A SIMPLE MODEL

MATTHEW NICHOLS

Sydney Institute for Astronomy, School of Physics, The University of Sydney, NSW 2006, Australia

DOUG LIN

Theoretical Astrophysics Santa Cruz (TASC), Department of Astronomy and Astrophysics, University of California, Santa Cruz, CA 95064, USA

AND

JOSS BLAND-HAWTHORN

Sydney Institute for Astronomy, School of Physics, The University of Sydney, NSW 2006, Australia

Draft version December 5, 2011

ABSTRACT

Dwarf galaxies in the Local Group appear to be stripped of their gas within 270 kpc of the host galaxy. Color-magnitude diagrams of these dwarfs, however, show clear evidence of episodic star formation ($\Delta t \sim$ a few Gyr) over cosmic time. We present a simple model to account for this behavior. Residual gas within the weak gravity field of the dwarf experiences dramatic variations in the gas cooling time around the eccentric orbit. This variation is due to two main effects. The azimuthal compression along the orbit leads to an increase in the gas cooling rate of $\sim ([1 + \epsilon]/[1 - \epsilon])^2$. The Galaxy's ionizing field declines as $1/R^2$ for $R > R_{\text{disk}}$ although this reaches a floor at $R \sim 150$ kpc due to the extragalactic UV field ionizing intensity. We predict that episodic SF is mostly characteristic of dwarfs on moderately eccentric orbits ($\epsilon > 0.2$) that do not come too close to the center ($R > R_{\text{disk}}$) and do not spend their entire orbit far away from the center ($R \gtrsim 200$ kpc). Up to 40% of early infall dwarf spheroidals can be expected to have already had at least one burst since the initial epoch of star formation, and 10% of these dwarf spheroidals experiencing a second burst. Such a model can explain the timing of bursts in the Carina dwarf spheroidal and restrict the orbit of the Fornax dwarf spheroidal. However, this model fails to explain why some dwarfs, such as Ursa Minor, experience no burst post-infall.

Subject headings: galaxies: dwarf — galaxies: evolution — galaxies: individual (Carina) — methods: analytical

1. INTRODUCTION

Dwarf galaxies, being some of the earliest collapsed structures in Λ CDM and hence representing potential building blocks of larger galaxies, have come to the forefront of studies of galactic evolution in recent years. The more than doubling of known Local Group dwarfs since the release of SDSS (York et al. 2000) has provided many more dwarfs in varying environmental situations to study. Despite most dwarfs being gas deficient within 270 kpc of the Galaxy (Grcevich & Putman 2009) they all show signs of ancient star formation potentially explaining this depletion of gas (Nichols & Bland-Hawthorn 2011). However, in addition to these ancient stellar populations many of these dwarfs around the Galaxy and within the Local Group show signs of distinct populations of younger stars arising from multiple starbursts separated by gigayears (Tolstoy et al. 2009; Weisz et al. 2011). For example, Fornax dwarf galaxy contains stars younger than 1 Gyr (Coleman & de Jong 2008). Paradoxically, there is little, if any, trace of molecular or atomic hydrogen to provide a sufficient reservoir of cool gas to enable the onset of star burst activities (Fornax shows only an off center cloud which may be Galactic gas, Carina with similar bursts shows no gas; Grcevich & Putman 2009).

These bursts of star formation are together responsi-

ble for, on average, 25% of the star formation within a dwarf (Lee et al. 2009) and may last for a period of time of order the dynamical time of the system (McQuinn et al. 2010b). These bursts occur with a large variation between dwarfs with some only experiencing one early burst of star formation, to Carina-like dwarfs with several distinct periods of star formation (Dolphin et al. 2005), to those that have continuous star formation with several to no small bursts (Weisz et al. 2011).

Stars formed over several generations also appear to have diverse heavy element abundance. The stellar metallicity distribution in many dwarfs is consistent with that expected from self contamination by early generations of massive stars, albeit with a substantial loss of supernova ejecta (Kirby et al. 2011a,b). In isolated dwarfs far from a massive spiral or elliptical galaxy, these bursts may be a consequence of gas being blown out and subsequently infalling with a time period of several gigayears (Dong et al. 2003; Valcke et al. 2008; Revaz et al. 2009). Episodic star formation in these isolated dwarfs require the gas that is blown out to remain bound. Otherwise if the dwarf is orbiting a host system, the gas could easily be blown outside of the Roche sphere to fall onto the host galaxy. Although radiatively driven outflow and tidal disruption may account for the lack of gas in these dwarf galaxies today, they also highlight the difficulties in gas retention and self contamination.

Here we present a simple self-consistent model that

may explain not only star bursts in non-isolated environments but also the lack of neutral gas in the dwarf galaxies around the Galaxy. We suggest gas is expelled after a star burst and subsequently reaccreted by its original host dwarf galaxies. This reaccretion process only occurs at the apogalacticon and any expelled gas that is not shielded from stripping by the dwarf is lost to the host.

2. MODEL

For a dwarf galaxy to successfully accrete gas at apogalacticon, the gas must stay within the dwarf's gravitational influence for a sufficiently long time to be allowed to cool and collapse before the tidal forces and ionizing radiation field are felt as the dwarf approaches perigalacticon.

The Roche sphere is the volume of space around the dwarf within which the dwarf's gravitational pull exceeds that of the Galaxy. At any point along the orbit the radius of the instantaneous Roche sphere is given by (King 1962)

$$r_{\text{RS}} = \left[\frac{Gm}{\omega^2 - d^2V/dR^2} \right]^{1/3}, \quad (1)$$

where r_{RS} is the radius of the Roche sphere, G the gravitational constant, m the mass of the dwarf, ω the angular velocity, V the potential of the Galaxy and R the Galactocentric radius.

At perigalacticon and apogalacticon in a Keplerian orbit, the size of the Roche sphere simplifies to

$$r_{\text{RS}}(R_{\text{peri}}) = R_{\text{peri}} \left[\frac{m}{M(3 + \epsilon)} \right]^{1/3}, \quad (2)$$

$$r_{\text{RS}}(R_{\text{apo}}) = \frac{1 + \epsilon}{1 - \epsilon} R_{\text{peri}} \left[\frac{m}{M(3 - \epsilon)} \right]^{1/3}, \quad (3)$$

where R_{peri} and R_{apo} is the radius of perigalacticon and apogalacticon respectively, M is the mass of the galaxy and ϵ the eccentricity of the orbit.

This increase in the Roche sphere, shown schematically in Figure 1, allows gas that is unbound at perigalacticon to be nominally bound at apogalacticon (assuming the momentum of the gas carries it through to apogalacticon). This gas is both compressed by the orbital path (by a factor of $[1 + \epsilon]/[1 - \epsilon]$) and experiences a weaker radiation field far out from the Galactic center. These factors allow the gas to cool and fall into the potential well of the dwarf triggering a starburst.

In order to participate in reaccretion, gas that is blown out must first survive an orbit of the Galaxy. This gas, which is likely to form small clouds once removed from the dwarf (Mayer et al. 2006), must survive the combination of high velocities and a strong radiation field at perigalacticon. For a cloud of gas with uniform density in hydrostatic equilibrium that is located directly behind the dwarf to survive an orbit with the same velocity as it began it must have an average distance, R_{cloud} , behind the dwarf of

$$R_{\text{cloud}} \sim \sqrt{\frac{2R_{\text{peri}}(1 + \epsilon)mr_{\text{cloud}}}{C_D M} \frac{T_{\text{halo}}}{T_{\text{cloud}}}}, \quad (4)$$

where r_{cloud} is the radius of the cloud, m and M are the masses of the dwarf and Galaxy respectively, T_{halo}

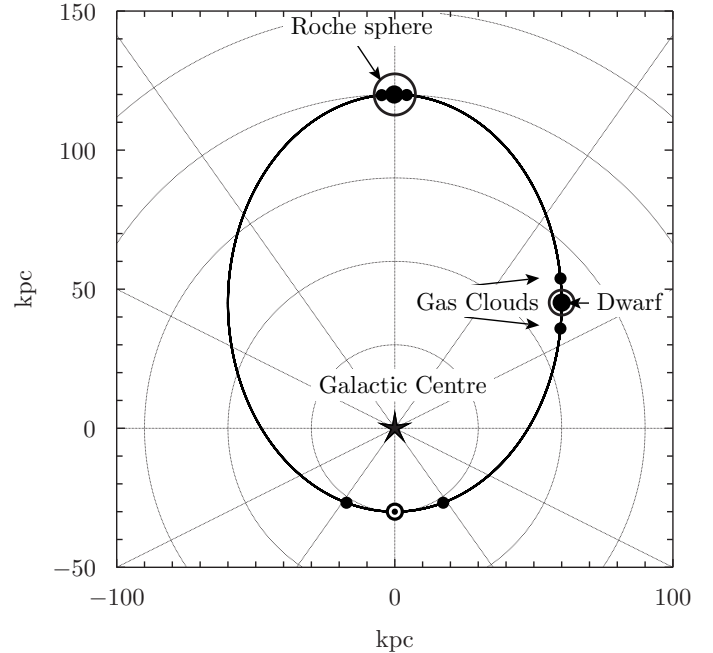


FIG. 1.— The change in Roche sphere over the orbit of a dwarf with a perigalacticon of 30 kpc and eccentricity of 0.6. The dwarf is represented by a solid circle in between two (smaller) solid circles representing gas clouds. The Roche sphere for a $3 \times 10^8 M_{\odot}$ dwarf around a $5.3 \times 10^{11} M_{\odot}$ galaxy is shown as a circle surrounding the dwarf at apogalacticon and at the mid-way point. At the perigalacticon the Roche sphere is shown as a white circle inside the point representing the dwarf galaxy. The Roche sphere changes from being able to encapsulate points at ± 50 Myr along the orbit to being an order of magnitude too small at perigalacticon. The orbital compression is visible by the changing spacing along the orbit, a consequence of Kepler's second law.

and T_{cloud} are the temperatures of the halo and cloud respectively and C_D is the coefficient of drag of the cloud (~ 1). Assuming that the mass ratio of the dwarf to the Galaxy is not too large, this value is comparable to the Roche sphere at perigalacticon. However, material off center may have to be much closer to the dwarf to experience the same level of protection from drag. The radius of survival will be increased by the dwarf's supersonic movement through the hot halo, and any turbulent wake behind the dwarf. These factors result in a much lower free-stream velocity (Neve & Shansonga 1989), and subsequently lower drag, behind the dwarf. As gas clouds behind rely on both the shock generated by the dwarf and the turbulent wake created by the dwarf's passage, a column of protection is formed behind the dwarf approximately the size of the Roche sphere dissipating at large distances. Gas clouds located in front of the dwarf will be slowed by drag until they are recaptured by the dwarf or they sink into the Galactic potential well. As gas clouds must be within the Roche sphere of the dwarf in order to be captured, a similar column of 'protection' (although in this case, a column of recapture) is located ahead of the dwarf. We therefore approximate the amount of material that is captured by the dwarf or survives an orbit as the amount of gas inside a column of radius equal to the Roche sphere at perigalacticon and along the orbital path of the dwarf.

Assuming that the bursts ionizes, heats, and expands gas within the dwarf such that it forms a uniform density sphere, then the amount of gas that will

be available at next apogalacticon is determined by the amount available at the previous apogalacticon. If the mass present in the last burst was $M_{\text{gas},i-1}$ then the sphere of gas post burst has a radius of $r_{g,i-1} = [(3M_{\text{gas},i-1})/(4\pi m_{\text{H}} n_{\text{H}})]^{1/3}$, where m_{H} is the mass of a hydrogen atom and n_{H} the density of hydrogen. If the post-burst density is constant, that is $n_{\text{H},i-1} = n_{\text{H},i}$ the only time this sphere can exceed the Roche sphere at apogalacticon is after the initial period of star formation, i.e. $r_{g,i} \leq r_{\text{RS}}(R_{\text{apo}})$, $i > 1$ since any additional gas would not have been accreted at the previous burst and could not be a component of this new sphere of gas.

Not all gas that fills this sphere will end up being redistributed after the next starburst. In addition to gas lost to stripping, some gas will also be consumed in the starburst ending up as the constituent stars. We assume the gas that ends up as stars to be approximately the mass in the Roche sphere at perigalacticon with this gas also possibly providing low level star formation throughout the orbit. This mass, chosen for analytic convenience, is—for most orbits—similar to the mass that would be consumed in a typical starburst given the gas consumption timescales and burst lengths (McQuinn et al. 2010a,b).

The radius in the warm sphere post burst is then

$$\frac{4}{3}\pi r_{\text{gas},i}^3 = 2\pi r_{\text{RS}}^2(R_{\text{peri}})r_{\text{gas},i-1} - 2\pi r_{\text{RS}}^3(R_{\text{peri}}),$$

$$r_{\text{gas},i} = r_{\text{RS}}(R_{\text{peri}}) \left[\frac{3}{2} \left(\frac{r_{\text{gas},i-1}}{r_{\text{RS}}(R_{\text{peri}})} - 1 \right) \right]^{1/3}, \quad (5)$$

with the volume of the Roche sphere at perigalacticon is altered by a factor of 3/2 to account for the difference in volume between a sphere and cylinder as $r_{\text{gas},i}/r_{\text{gas},i-1} \rightarrow 1$.

As this gas is expelled from the dwarf by the starburst, it will quickly be heated to a warm phase of around $T = 10^4$ K. This gas will be moving through an isothermal exponential hot halo of gas with a hydrogen density (n_{H}) of $n_{\text{H}} \sim 3 \times 10^{-4} \text{ cm}^{-3}$ at 50 kpc consistent with Bland-Hawthorn et al. (2007). The gas is assumed to consist of small clouds in hydrostatic equilibrium with a hot halo. The mean density of hydrogen around the dwarf galaxy is assumed to be $n_{\text{H}} \sim 10^{-3} \text{ cm}^{-3}$, a filling factor of $\sim 10\%$ at distances of 150 kpc. This gas will be easy to see in absorption through QSO sight lines but unable to be seen in emission. For this low density gas to participate in the next starburst it must first fall back into the central gravitational potential and cool into a neutral cold phase.

For a low metallicity gas, $[\text{Fe}/\text{H}] = 0.1$, at these densities the cooling timescale is $t_{\text{cool}} \sim 30$ Myr (Sutherland & Dopita 1993). The cooling time will be slightly larger than the values given here due to the need to radiate energy gained from the collapse and the heating effect of the radiation fields. The timescale of infall can be over an order of magnitude larger $t_{\text{infall}} \sim 300$ Myr. This timescale is comparable to the timescale of a typical burst of a few hundred megayears (Lee et al. 2009; McQuinn et al. 2010b) and may influence how long the burst occurs for. These timescales however, are all much shorter than the orbital timescale of a few gigayear which determines how rapidly the Roche sphere changes.

This short timescale for cooling can only occur at apogalacticon. At perigalacticon the gas will be extended

along the orbital path according to Kepler's second law, lowering its density by a factor of $(1+\epsilon)/(1-\epsilon)$ and hence increasing its cooling time by a factor of $[(1+\epsilon)/(1-\epsilon)]^2$. In addition the gas experiences a much stronger radiation field which will counteract any cooling and reassociation taking place, leaving most gas ionized until apogalacticon.

As the gas cools and falls into the center of the potential well of the dwarf, increased radiation from the Galaxy will be the major factor preventing a burst. In addition to this Galactic radiation field, the dwarf will also experience the extragalactic UV background.

As star formation requires optically thick gas to occur, all ionizing photons from the Galactic field are assumed to be absorbed, with the Galactic field dropping off as an inverse square law, with the (opacity corrected) photon flux given by (Bland-Hawthorn & Maloney 1999, 2002)

$$\varphi = \frac{2.7 \times 10^8}{(R \text{ kpc})^2} \frac{\text{SFR}(t)}{\text{SFR}(t_{\text{now}})} \text{ photons cm}^{-2} \text{ s}^{-1}. \quad (6)$$

We use the time varying extragalactic UV field derived by Faucher-Giguère et al. (2009), with the absorption of this radiation is done according to the prescription in (Sternberg et al. 2002) with a constant density neutral core surrounded by an ionized medium of equal density.

3. RESULTS

The timing of apogalacticons—and consequently bursts in this model—is determined by the orbital properties of the dwarf. Two models are investigated, that of a simple Keplerian system described by equations (2) and (3) and of point masses orbiting inside a growing Einasto halo. Both systems consists a dwarf with a point mass $m = 1 \times 10^9 M_{\odot}$, a value consistent with the virial mass of a dwarf that formed at $z \sim 10$ and possesses a dynamical mass similar to that observed in dwarf galaxies today within 300 pc of the dwarf's center (Strigari et al. 2008). Each dwarf has an initial gas mass of $1.5 \times 10^8 M_{\odot}$ consistent with the universal baryon to dark matter ratio.

Inside the Keplerian system the dwarfs orbit a host Galaxy of mass $M = 5.3 \times 10^{11} M_{\odot}$. This mass is roughly half that of the virial mass of the Milky Way, but is consistent with the mass of the halo within 100 kpc that reaches the same virial mass at the Milky Way derived from the RAVE survey (Smith et al. 2007). These dwarf galaxies begin at apogalacticon 12 Gyr ago, and experience a burst at every future apogalacticon.

For dwarfs inside a growing Einasto halo, a $z = 0$ virial mass of $1.4 \times 10^{12} M_{\odot}$ is assumed, consistent with the circular velocity from the RAVE survey. The mass of this halo is calculated backward in time by assuming the median rate of growth for Milky Way size dark matter halos within the Millennium-II simulation (Boylan-Kolchin et al. 2010). Dwarf galaxies inside the growing Einasto halo are assumed to be at perigalacticon today and traced back in time 10 Gyr. Beginning dwarfs at apogalacticon assures that only dwarfs which can have completed one full orbit of the Milky Way will be calculated to have undertaken a burst.

By calculating the total amount of gas available from equation (5) and the amount of this gas that is ionized the mass available to fuel each starburst is able to be calculated as a function of perigalacticon and eccentric-

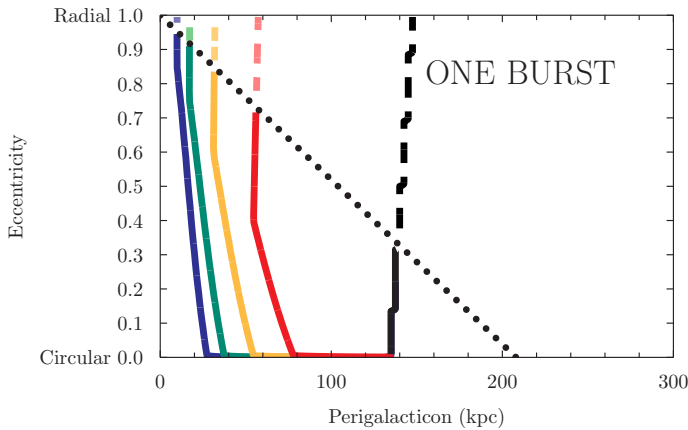


FIG. 2.— The orbit properties (perigalacticon radius versus orbital eccentricity) of dwarf galaxies that retain sufficient gas to experience a burst of star formation post initial star formation in a Keplerian model with dwarf galaxy of mass $10^9 M_\odot$ and Galaxy point mass of $5.3 \times 10^{11} M_\odot$. The solid contours (left to right and blue to red in online version) correspond to gas masses of 1, 3, 10 and $30 \times 10^6 M_\odot$ at the time of the first burst. The dashed contours (light colors in online version) correspond to dwarfs that have yet to experience a burst of star formation but are expected to have sufficient gas to cause one in the future. The dashed black line shows the upper limit of perigalacticons which experience bursts of any gas mass. Beyond this, we consider dwarfs to be isolated, with a large Roche sphere that only slowly evolves. Above the dotted line the orbit times exceed the age of the universe.

ity. Many dwarfs are able to experience at least one burst subsequent to initial star formation, the mass available in the Keplerian system is shown in Figure 2, with dwarfs on approximately circular orbits far away experiencing the biggest bursts, a consequence of their large perigalacticon Roche sphere. Assuming that the star formation rate in the Galaxy and the extragalactic UV background are constant into the future, the amount of gas available at a future burst is also able to be easily calculated for the Keplerian system.

Similar contours are seen within the growing Einasto halo with the amount of gas available shown in Figure 3. The more complicated structure seen in the Einasto halo dwarfs arises from the variable orbits inside a growing halo. As dwarfs will experience varying peri- and apogalacticons as the halo grows and decreasing Roche spheres the amount of gas available for bursts can change greatly for slight variations in perigalacticon and eccentricity. This effect is greatly increased when orbits are traced back beyond 10 Gyr and the dwarf to halo mass ratio becomes larger.

At the second burst—the third period of star formation—the amount of dwarfs with large amounts of neutral gas ($M_{\text{gas}} > 10^6 M_\odot$) is greatly decreased, Figure 4 for Keplerian system dwarfs and Figure 5 for Einasto system dwarfs, with those at low pericentre not able to hold onto sufficient amounts of gas, and those at large pericentre not having enough time to undergo multiple bursts. These dwarfs may be able to undergo future bursts if given enough time, and assuming the ionization field is similar to that which exists today. These regions nearly completely disappear by the third burst with very few dwarfs able to have completed three orbits and be far enough away to not be ionized by the Galaxy.

The star formation rate of a burst can be calculated by

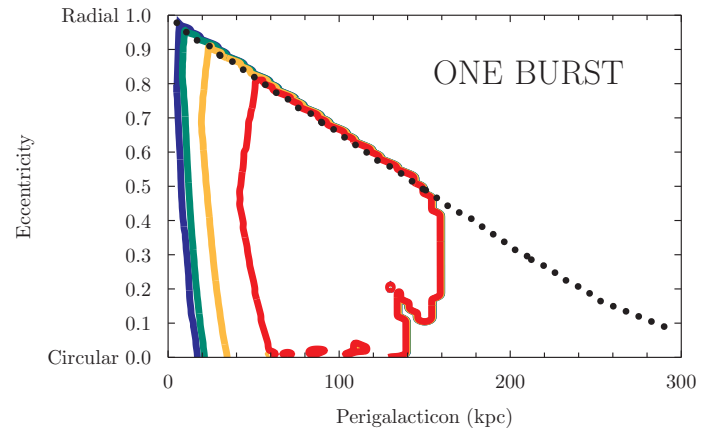


FIG. 3.— The orbit properties (perigalacticon radius versus orbital eccentricity) of dwarf galaxies that retain sufficient gas to experience a burst of star formation post initial star formation in an Einasto halo. The contours are detailed in Figure 2. To the right of the red contour dwarfs have slowly evolving large Roche spheres and may be considered isolated. Above the dotted line the orbit time of dwarfs which are at perigalacticon today is longer than 10 Gyr.

the amount of neutral hydrogen present within a dwarf, with the star formation rate in dwarfs being able to be approximated as a power law of the neutral gas mass $\text{SFR} \propto M_{\text{HI}}^{1.4}$ (Kaisin & Karachentsev 2006). As the second burst has less gas, a consequence of equation (5), this rate of star formation nearly always decreases, a consequence of the gas being lost throughout the orbit. Assuming that each burst is undertaken for an equal period of time, the ratio of the strength of the first to second burst can be calculated. This ratio, also shown in Figures 4 and 5, is typically about three to one increasing as orbits become more radial ($\epsilon \rightarrow 1$). This ratio always exceeds unity for dwarfs with over $10^6 M_\odot$ of HI available for star formation but can be less for close in, nearly circular orbits which have smaller amounts of gas available. Dwarfs that have large amounts of gas ionized, that is dwarfs with a low apogalacticon occurring close at a time of heightened Galactic star formation, will not undergo a burst and may be able to hold onto more gas for future bursts than calculated. This ionized gas will however, be more susceptible to stripping and will still have gas loss throughout the orbit.

The ability to calculate the relative strength of bursts allows a comparison to the star formation of known dwarfs such as Carina.

Assuming a common infall time of 12 Gyr (consistent with early infalling dwarfs who will have experienced multiple orbits of the Galaxy Rocha et al. 2011) and using orbit distribution results from N -body distributions (Wetzel 2011) we calculate the proportion of dwarfs that have experienced a first, second or third burst.

Around a Milky Way sized halo, up to 25% of early infalling dwarfs in a Keplerian system should have experienced at least one burst with over $10^6 M_\odot$ of gas available. A third of these dwarfs, 9% of all early infalling dwarfs will have experienced two such bursts, while no dwarfs today are expected to have undergone three bursts of such magnitudes with any individual dwarf having only a 1% chance of having completed three orbits each with a burst in the age of the Universe.

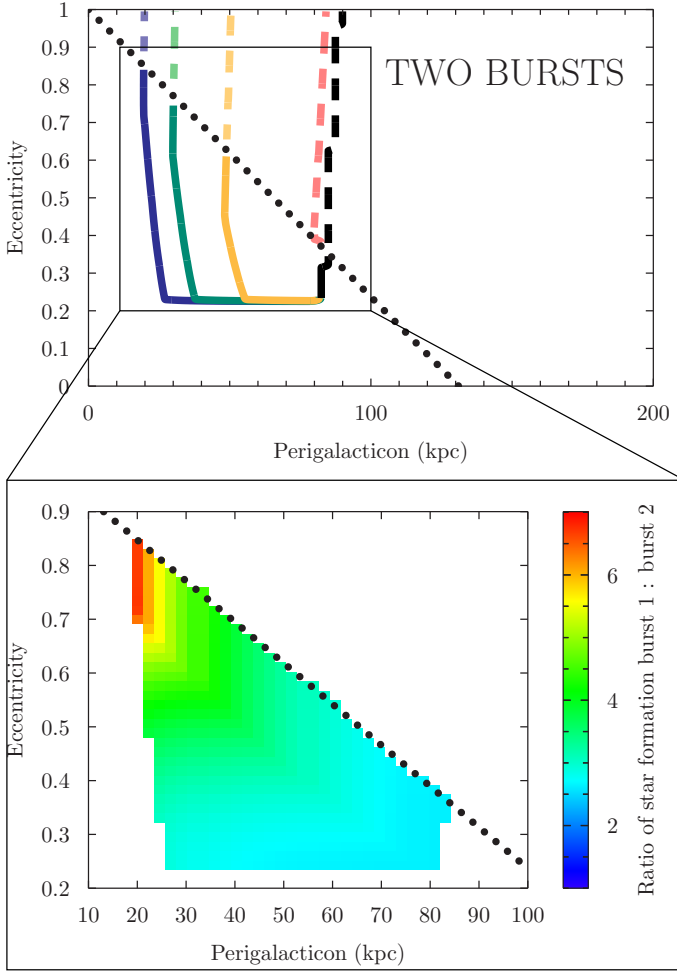


FIG. 4.— The orbit properties (perigalacticon radius versus orbit eccentricity) that retain sufficient gas to experience a *second* burst of star formation in a Keplerian model. The contours are detailed in Figure 2. Above the dotted line orbit times exceed half the age of the universe. The zoomed graph underneath shows the ratio of star formation that occurred in the first to the second burst in dwarfs that will have experienced two bursts today with at least $10^6 M_{\odot}$ of gas.

Within a more realistic growing Einasto halo, up to 40% of early infall dwarfs will have experienced at least one burst (this figure may be higher still due to the tendency for orbits to have higher periapsis inside extended halos Wetzel 2011), half of these 17% will have experienced two such bursts subsequent to initial star formation and 1.5% three such bursts.

Late infalling dwarfs may have bursts of star formation that occurred when isolated from the hot halo environment (e.g. Leo I is likely to have had a burst of star formation at or before its recent infall Rocha et al. 2011), and if falling in gas rich, only have undertaken this mechanism of bursts once if at all.

4. THE CASE OF CARINA AND FORNAX

The Carina dwarf spheroidal has three distinct periods of rapid star formation, separated by ~ 5 Gyr. Carina is also likely to have undergone many apogalacticons, with a pericentre of $R_{\text{peri}} = 50 \pm 30$ kpc and apocentre of $R_{\text{apo}} = 110 \pm 30$ kpc (Lux et al. 2010; Pasetto et al. 2011). A number of orbits satisfy these constraints with

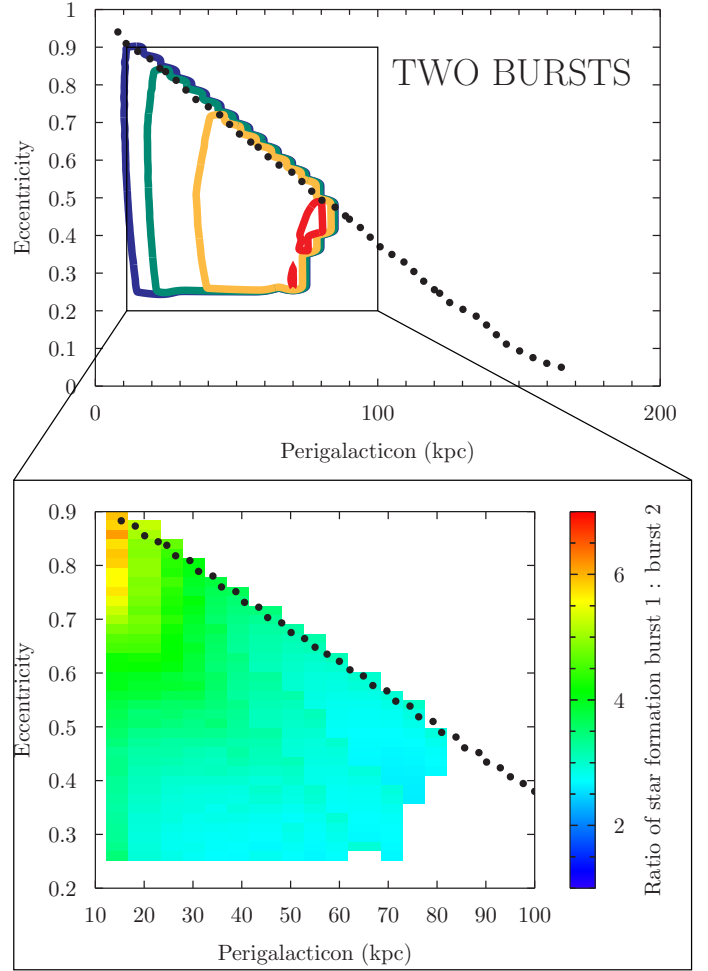


FIG. 5.— The orbit properties (perigalacticon radius versus orbit eccentricity) that retain sufficient gas to experience a *second* burst of star formation in an Einasto model. The contours are detailed in Figure 2. Above the dotted line orbit times are long enough that dwarfs at perigalacticon today could not have completed two orbits in 10 Gyr. The zoomed graph underneath shows the ratio of star formation that occurred in the first to the second burst in dwarfs that will have experienced two bursts today with at least $10^6 M_{\odot}$ of gas.

bursts at apogalacticons occurring near the bursts in star formation of Carina and consistent with an infall time 7–9 Gyr derived by Rocha et al. (2011). All these orbits have an apogalacticon in between the bursts of Carina, however, the length of Carina's first burst (second period of star formation) is comparable to the orbital period of Carina which will have prevented gas from cooling and fueling another burst immediately. The allowed orbits, shown in Figure 6 vary depending on if Carina has just passed or is just about to pass an apogalacticon (both are consistent with the radial velocity of Carina Piatek et al. 2003).

A greater constraint can be applied assuming that Carina's star formation rate would have consumed the gas within a Hubble time had it not been interrupted. Such a timeframe is consistent with the star formation rates of gas rich dwarfs in the Local Group Kaisin & Karachentsev (2006). To achieve the $\sim 0.004 M_{\odot} \text{ yr}^{-1}$ rate calculated by Hurley-Keller et al. (1998), Carina must have had $\sim 5 \times 10^7 M_{\odot}$ of neutral hydrogen available. As-

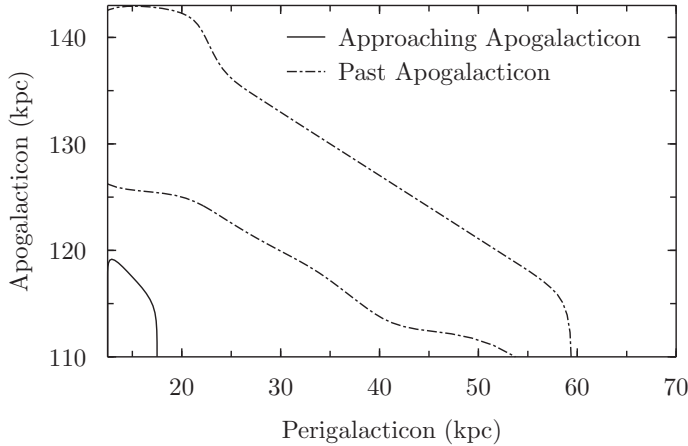


FIG. 6.— The allowed orbits of Carina which produce two bursts containing over $10^6 M_\odot$ and have the first and third apogalacticon within 500 Myr of the start of the bursts derived in Hurley-Keller et al. (1998). The second apogalacticon is unlikely to have a burst due to the long period of star formation occurring at the first burst, which occurs over an entire orbit. Extending the allowed variation of bursts to ± 1000 Myr greatly increases the allowed parameter space of the orbits.

suming that Carina has a dark matter mass of $10^9 M_\odot$ and began with 15% of this mass in Hydrogen (consistent with the universal baryon to dark matter fraction) Assuming a dark matter mass of $10^9 M_\odot$ and 15% gas content (consistent with the universal baryonic fraction) only the high pericentre orbits have this amount of material available for star formation, however, such orbits are also up to a Gyr out of time with the estimates of Carinas bursts. It must be noted however, that the gas consumption timescales differ by an order of magnitude and hence Carina could conceivably be on any of these orbits.

This method can be extended to other dwarf spheroidals such as Fornax, see Figure 7, under such a model Fornax infall must have been towards the upper limit of ~ 8 Gyr found by (Rocha et al. 2011). However, this method clearly fails when applied to Ursa Minor dwarf which has one ancient period of star formation and no bursts post-infall (Rocha et al. 2011). This is despite some allowed orbits of Ursa Minor predicted to have three bursts of star formation, this indicates that the protection of gas clouds by the dwarf may be overstated by this simple model.

5. CONCLUSION

We have presented a model for star formation bursts inside dwarf galaxies orbiting a host galaxy. Under this model fall back of gas into the potential well of dwarf galaxies will occur at apogalacticon and allow episodic star formation for non-isolated dwarfs. This model predicts that dwarfs with more than one burst today will be at a moderate perigalacticon from the host galaxy and of moderate eccentricity. The second burst (the third period of star formation) is expected to be two to four times weaker than the first burst that follows initial star formation for most dwarfs. This second burst may not have yet occurred in some dwarfs which, with a higher perigalacticon, may be expected to undergo another burst at a future point. For dwarfs near apogalacticon and on the verge of experiencing their first or second burst

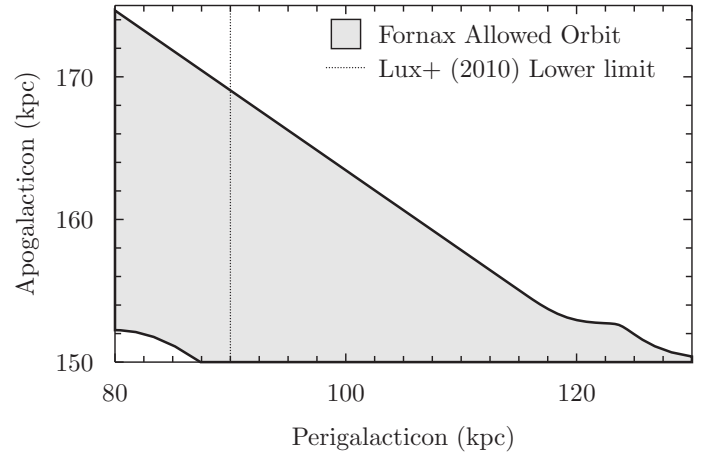


FIG. 7.— The orbital range for which Fornax will have had only one burst with $> 10^6 M_\odot$ of gas available between 3.5 and 4.5 Gyr ago. Combined with the lower perigalacticon limit from Lux et al. (2010) the allowed range is significantly reduced.

of star formation we predict that low columns of diffuse ionized gas will be present in the vicinity of the dwarfs. Such gas although much too faint to be seen in emission should have sufficient column to be detectable in absorption along QSO sight lines. In particular this infalling gas should appear in recently infalling ($\lesssim 5$ Gyr) dwarfs that are now near apogalacticon. Leo II is possibly the best candidate for this search. Lépine et al. (2011) in calculating the proper motion suggest it is near either perigalacticon or apogalacticon, we would take the stronger view that due to its deficiency in gas (Knapp et al. 1978) and the difficulty of stripping at such large radii (Nichols & Bland-Hawthorn 2011) as well as the longer time spent at larger radii that it is near apogalacticon. When combined with a recent infall (Rocha et al. 2011) and the abundance of extragalactic sources (Lépine et al. 2011) Leo II becomes a good candidate for QSO sight lines picking up any warm gas infalling onto the dwarf. Although Fornax is not near its expected apogalacticon (Lux et al. 2010) the offset hydrogen feature although possibly Galactic gas (Grcevich & Putman 2009) and numerous QSO sight lines (Tinney 1999) would be worth investigating.

Dwarfs that have experienced no burst yet in this model, may be isolated enough to allow gas expelled from initial star formation to fall back into the dwarf triggering another burst (Dong et al. 2003) and may have multiple bursts already, this process is unlikely to have happened in dwarfs that have already experienced one orbit of the Galaxy.

This model is able to explain the magnitude of the star formation bursts inside the Carina dwarf spheroidal, however, it cannot explain the timing of the bursts with some mechanism required to suppress star formation at an apogalacticon without stripping gas between the observed bursts. This may simply be that the gas clouds only fall in closer at the first apogalacticon, before drag prevents accretion until the next apogalacticon. The differing size of dwarf galaxy dark matter halos will also impact the results, with less massive halos less able to retain their gas against ram pressure stripping throughout the orbit. Dwarf spheroidals with more massive halos would then be more likely to have experienced multiple

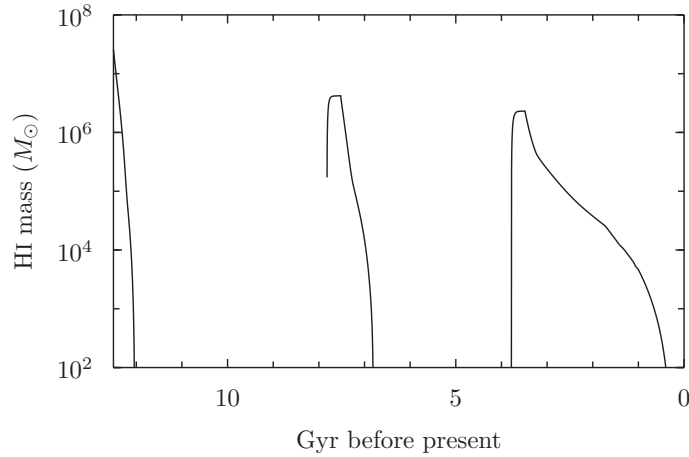


FIG. 8.— Reaccretion added to Nichols & Bland-Hawthorn (2011) with cold gas added over 300 Myr after apogalacticon.

bursts of star formation.

As dwarfs that lose gas are likely to do so as gas clouds of not insignificant mass (Mayer et al. 2006) there will be a large amount of variation as to how many clouds have managed to fall in by the beginning of star formation, and could result in a second burst being larger than the first. This model is able to be easily applied to non-Keplerian and time-varying orbits such as Einasto halo dwarf galaxies within a growing halo around the Galaxy

at the cost of requiring the orbits and equations to be solved numerically.

D.C.L. is grateful to the University of Sydney for hosting him during the preparation of this paper. J.B.-H. is supported by a Federation Fellowship from the Australian Research Council.

APPENDIX

REACCRETION WITH EARLY INTERNAL HEATING

The expulsion of gas from a dwarf is not automatic, and is helped greatly by internal heating assisted ram pressure stripping (Nichols & Bland-Hawthorn 2011). Under instantaneous ram pressure stripping this gas, once lost, eventually ends up in the host. However, gas once removed from the main body will experience less drag (arising from ram pressure) as the free stream velocity is reduced both by the dwarf galaxies shock and by the turbulent wake behind. Even gas which is unbound at perigalacticon but sufficiently close may maintain enough momentum to later be reaccreted when far from the Galaxies center. This gas can be modelled in the Nichols & Bland-Hawthorn (2011) case by the addition of cold gas after an apogalacticon (over a suitable period of time, dependent upon the freefall time) with the magnitude dictated by the above model. A simple case of this is a Carina like orbit modelled from $z = 5$ is shown in Figure 8. In this case, gas was added at the appropriate apogalacticons to simulate a Carina like burst. The additional amount of gas added at the second period of star formation (the first burst) was quickly lost, this is due to the short period of time over which gas is added (300 Myr) and the stronger external radiation field present. Although the first and second burst initially begin losing gas at the same rate, once mass is lost, the external radiation field has a larger effect on the first burst, resulting in a much more rapid gas loss than the second burst.

REFERENCES

- Bland-Hawthorn, J., & Maloney, P. R. 1999, *ApJ*, 510, L33
 Bland-Hawthorn, J., & Maloney, P. R. 2002, in *Astronomical Society of the Pacific Conference Series*, Vol. 254, *Extragalactic Gas at Low Redshift*, ed. J. S. Mulchaey & J. T. Stocke, 267–
 Bland-Hawthorn, J., Sutherland, R., Agertz, O., & Moore, B. 2007, *ApJ*, 670, L109
 Boylan-Kolchin, M., Springel, V., White, S. D. M., & Jenkins, A. 2010, *MNRAS*, 406, 896
 Coleman, M. G., & de Jong, J. T. A. 2008, *ApJ*, 685, 933
 Dolphin, A. E., Weisz, D. R., Skillman, E. D., & Holtzman, J. A. 2005, *ArXiv Astrophysics e-prints*
 Dong, S., Lin, D. N. C., & Murray, S. D. 2003, *ApJ*, 596, 930
 Faucher-Giguère, C., Lidz, A., Zaldarriaga, M., & Hernquist, L. 2009, *ApJ*, 703, 1416
 Greевич, J., & Putman, M. E. 2009, *ApJ*, 696, 385
 Hurley-Keller, D., Mateo, M., & Nemec, J. 1998, *AJ*, 115, 1840
 Kaisin, S. S., & Karachentsev, I. D. 2006, *Astrophysics*, 49, 287
 King, I. 1962, *AJ*, 67, 471
 Kirby, E. N., Cohen, J. G., Smith, G. H., Majewski, S. R., Sohn, S. T., & Guhathakurta, P. 2011a, *ApJ*, 727, 79
 Kirby, E. N., Martin, C. L., & Finlator, K. 2011b, *ApJ*, 742, L25
 Knapp, G. R., Kerr, F. J., & Bowers, P. F. 1978, *AJ*, 83, 360
 Lee, J. C., Kennicutt, R. C., José G. Funes, S. J., Sakai, S., & Akiyama, S. 2009, *ApJ*, 692, 1305
 Lépine, S., Koch, A., Rich, R. M., & Kuijken, K. 2011, *ApJ*, 741, 100
 Lux, H., Read, J. I., & Lake, G. 2010, *MNRAS*, 406, 2312
 Mayer, L., Mastropietro, C., Wadsley, J., Stadel, J., & Moore, B. 2006, *MNRAS*, 369, 1021
 McQuinn, K. B. W., et al. 2010a, *ApJ*, 721, 297
 —. 2010b, *ApJ*, 724, 49
 Neve, R., & Shansonga, T. 1989, *International Journal of Heat and Fluid Flow*, 10, 318
 Nichols, M., & Bland-Hawthorn, J. 2011, *ApJ*, 732, 17
 Pasetto, S., Grebel, E. K., Berczik, P., Chiosi, C., & Spurzem, R. 2011, *A&A*, 525, A99+
 Piatek, S., Pryor, C., Olszewski, E. W., Harris, H. C., Mateo, M., Minniti, D., & Tinney, C. G. 2003, *AJ*, 126, 2346
 Revaz, Y., et al. 2009, *A&A*, 501, 189
 Rocha, M., Peter, A. H. G., & Bullock, J. S. 2011, *ArXiv e-prints*

- Smith, M. C., et al. 2007, MNRAS, 379, 755
Sternberg, A., McKee, C. F., & Wolfire, M. G. 2002, ApJS, 143, 419
Strigari, L. E., Bullock, J. S., Kaplinghat, M., Simon, J. D., Geha, M., Willman, B., & Walker, M. G. 2008, Nature, 454, 1096
Sutherland, R. S., & Dopita, M. A. 1993, ApJS, 88, 253
Tinney, C. G. 1999, MNRAS, 303, 565
Tolstoy, E., Hill, V., & Tosi, M. 2009, ARA&A, 47, 371
Valcke, S., de Rijcke, S., & Dejonghe, H. 2008, MNRAS, 389, 1111
Weisz, D. R., et al. 2011, ApJ, 739, 5
Wetzel, A. R. 2011, MNRAS, 412, 49
York, D. G., et al. 2000, AJ, 120, 1579